OMP Decarboxylase: The Reaction Mechanism and the

Binding of an Isosteric Inhibitor

By

Brian J. DelFraino

Submitted in Partial Fulfillment of the Requirements for the Degree of Masters of

Science in the Chemistry Program

YOUNGSTOWN STATE UNIVERSITY

December, 2003

OMP Decarboxylase: The Reaction Mechanism and the

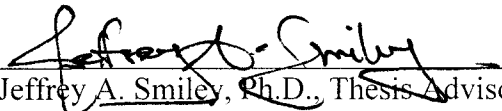Binding of an Isosteric Inhibitor

Brian J. DelFraino

I hereby release this thesis to the public. I understand this thesis will be made available from the OhioLink ETD Center and the Maag Library Circulation Desk for public access. I also authorize the university or other individuals to make copies of this thesis as needed for scholarly research.

Signature:

_____   12/08/03
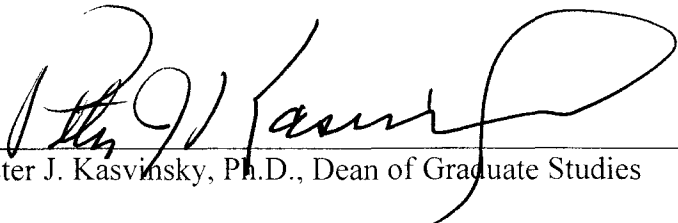Brian J. DelFraino   Date

Approvals:

_____
Jeffrey A. Smiley, Ph.D., Thesis Advisor   Date

_____   12/8/03
Michael A. Serra, Ph.D., Committee Member   Date

_____   12/8/03
John A. Jackson, Ph.D., Committee Member   Date

_____   12/9/03
Peter J. Kasvinsky, Ph.D., Dean of Graduate Studies   Date

Abstract

Orotidylate decarboxylase (ODCase) is the final enzyme in the *de* novo biosynthetic pathway of pyrimidine biosynthesis. The chemical mechanism by which ODCase catalyzes the formation of uridylate (UMP) to orotidylate (OMP) is not yet apparent since it follows no common decarboxylation routes. Our group has suggested a model for this decarboxylation that involves proton donation to the transition state in a concerted ylide/zwitterions mechanism. Yeast ODCase was purified of any contaminating proteins. Complete synthesis and characterization of transition-analogues was performed which act and were used as inhibitors to explore the enzyme active site. 1H NMR of spectroscopy of ODCase in complex with 6-thiocarboxamidoruidine-5′-monophosphate reveals a new downfield signal, possible identifying hydrogen bonds between the enzyme and the inhibitor. Our proposed catalytic mechanism and the results obtained from the experiment are to be discussed in this thesis.

Acknowledgements

I wish to express my love and gratitude to my parents and family who provided support, patience and wisdom to me in all my endeavors, especially my mother, whose love, support, criticisms, and sacrifices have allowed me to become the person I am today. My warmest wishes go out to Dan, Vince, Katie, KT, Vanessa, and Craig who became some of my closest friends and provided the most interesting of conversation day in and day out. I'd also like to thank my D&D group and best friends Mark, Mike, Bob, Tom, Morris and Chris who provided the stress relief I needed throughout the week every Wednesday night.

I would also like to thank my advisor and friend Dr. Jeffrey Smiley for his guidance in the lab. When I faltered, and I did, he showed me the utmost patience and support where others would have given up. He helped develop, in me, a love of science and research and has provided me the tools I need to continue my career. My recognition goes out to all my professors, especially Dr. John Jackson and Dr. Michael Serra who reviewed this thesis. Lastly, I would like to thank the Department of Chemistry at Youngstown State University for giving me the opportunity to purse a Master's degree.

Table of Contents

Table of Contents (Continued)

List of Figures

List of Symbols and Abbreviations

α	alpha
β	beta
g	gram
L	liter
EI-MS	Electrospray Ionization Mass Spectrometry
M	molarity
μ	micro-
MHz	megahertz
min	minute
mol	mole
mL	mL
nm	nanometer
NMR	nuclear magnetic resonance
°C	degrees Centigrade
ppm	parts per million
rpm	revolutions per minute
TLC	thin layer chromatography
UV	ultraviolet
v/v	volume by volume
w/v	weight by volume
λ	wavelength

Chapter 1: Introduction

Nucleotides are biological molecules, possessing heterocyclic nitrogenous bases as principle components of their structure. Their roles are numerous, many serving as intermediates in most aspects of cellular metabolism. These include regulation of cell metabolism and function, energy conservation and transport, formation of coenzymes and active intermediates of phopholipid and carbohydrate metabolism and formation of the essential building blocks of both deoxyribonucleic acid (DNA) and ribonucleic acid (RNA).

Nucleotides are present in two distinct forms: pyrimidines and purines. Pyrimidines, such as cytosine, thymine and uracil, are six-membered heterocyclic aromatic rings containing two nitrogen atoms. Purines, these include guanine and adenine, are represented by the combination of a pyrimidine ring with a five-membered, imidazole ring yielding a fused ring system.

The *de novo* pyrimidine biosynthetic pathway (Scheme 1), through which pyrimidine ribonucleotide biosynthesis occurs, was described in a review by Mary Ellen Jones.[1] This biosynthetic process is a six-step, channeled series of reactions. Intermediates are not released into the medium but rather moved from one enzyme to the next.[2] In contrast to purines, pyrimidines ring systems are completed prior to the addition of the ribose-5-phosphate moiety as opposed to being synthesized as nucleotide derivatives. The process begins with the enzyme carbamoyl phosphate synthatase II (CPS II) combining the amino acid glutamine, water and a carbonate ion to yield carbamoyl
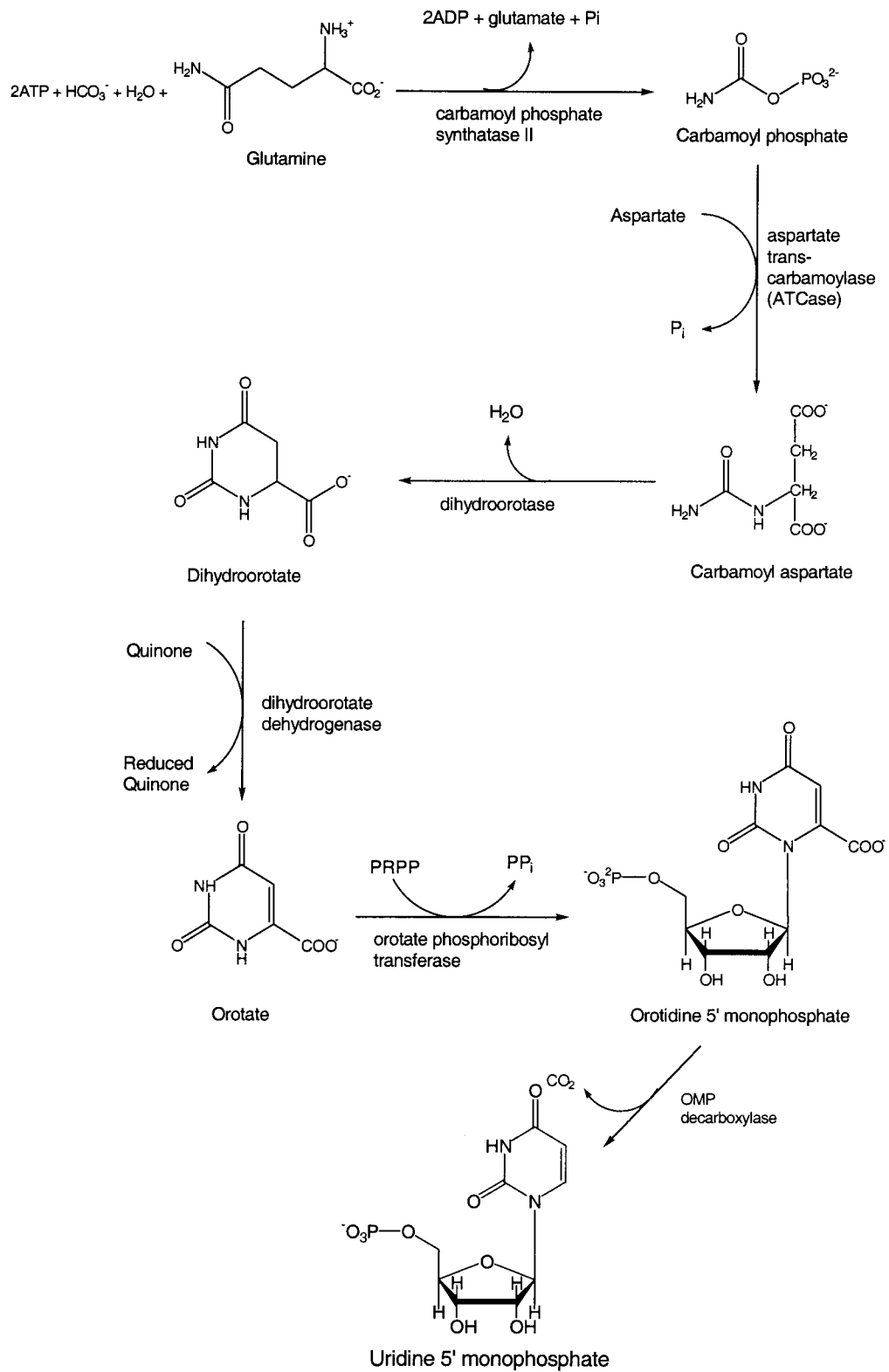
Scheme 1: Pyrimidine Biosynthesis Pathway.

phosphate. In this step, two molecules of adenosine triphospate (ATP) are required. The

first phosphate provides a phosphate group to the molecule and the second provides the

necessary energy to drive the reaction forward. The second enzyme, aspartate

transcarbamoylase (ATCase) then catalyzes the condensation of carbamoyl phosphate

with aspartate to form carbamoyl aspartate. Note that no ATP is required because the

carbamoyl phosphate is found in an "active" form. The enzyme, dihydroorotase then

directs a ring closer and dehydration of carbamoyl aspartate via linkage of the $-NH_2$

group of the carbamoyl phosphate with the former β-COO$^-$ of aspartate to give

dihydroorotate and water. Dihydroorotate is then oxidized by the enzyme dihydroorotate

dehydrogenase yielding orotate, a true pyrimidine, along with reduced quinone, an

electron acceptor. A ribose monophosphate is added to orotate by the enzyme orotate

phosphoribosyl transferase to form orotidine-5'-monophosphate (OMP). The final step is

the decarboxylation of OMP by the enzyme orotidylate-5'-decarboxylase (ODCase) to

produce uridine-5'-monophosphate (UMP), one of the two common pyrimidine

ribonucleotides.

Decarboxylation reactions are a process by which the displacement of a carboxyl

group occurs by the addition of a proton with the formation of an anion intermediate

(often an enolate) where the reaction rates are mediated by the stability of the anion

intermediate (Scheme 2).

$$\underset{R}{\overset{O}{\underset{}{\parallel}}}\!\!-\!\!O^- + H^+ \rightleftharpoons R^- + H^+ + CO_2 \rightleftharpoons R-H + CO_2$$
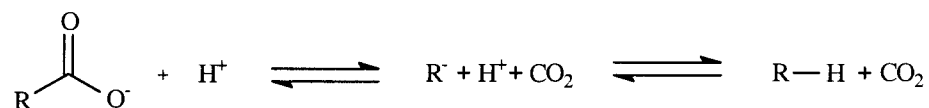
Scheme 2: General decarboxylation equation.

There are four general types of decarboxylation reactions, all of which can be described by either the substrate or the mechanism present. These types are α-keto acid/thiamin pyrophosphate (TPP), β-keto acid/metal ion, amino acid/pyridoxal (pyruvate) and β-OH acid/oxidative decarboxylations.[3] α-Keto acid/TPP decarboxylations occur in the presence of both a cofactor and metal ion. Cofactors are metal ions or organic molecules that are actively involved in the catalytic reaction of enzymes.
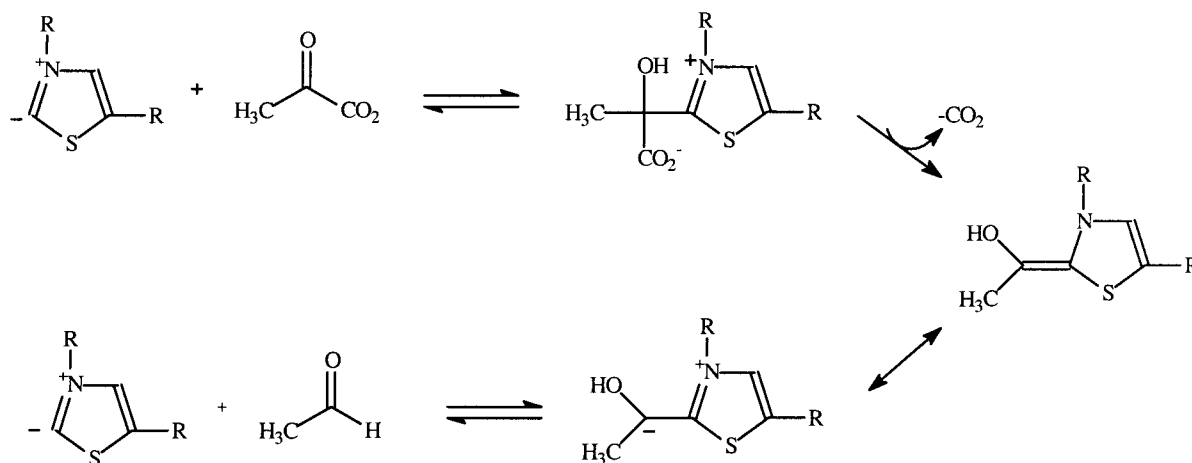
Scheme 3: Mechanism of the decarboxylation of pyruvate by TPP

They often serve as intermediate carriers of functional groups in the conversion of substrate to product. α-Keto acid decarboxylations require both the cofactor thiamin pyrophosphate (TPP), and a divalent metal ion. One example of this type of decarboxylation is found in the decarboxylation of pyruvic acid to yield carbon dioxide and acetaldehyde.[4] (Scheme 3)

β-Keto acid/metal ion decarboxylations (Scheme 4) are quite similar to α-keto

acid decarboxylations, requiring a divalent metal ion for catalysis. However, these types

of decarboxylations do not require a cofactor, such as TPP, in order to proceed. An

example of this type of decarboxylation can be seen in oxaloacetate decarboxylase. Here,

enzyme bound metal chelates to the α-carboxyl and keto carbonyl of the substrate prior

to decarboxylation.[5,6]
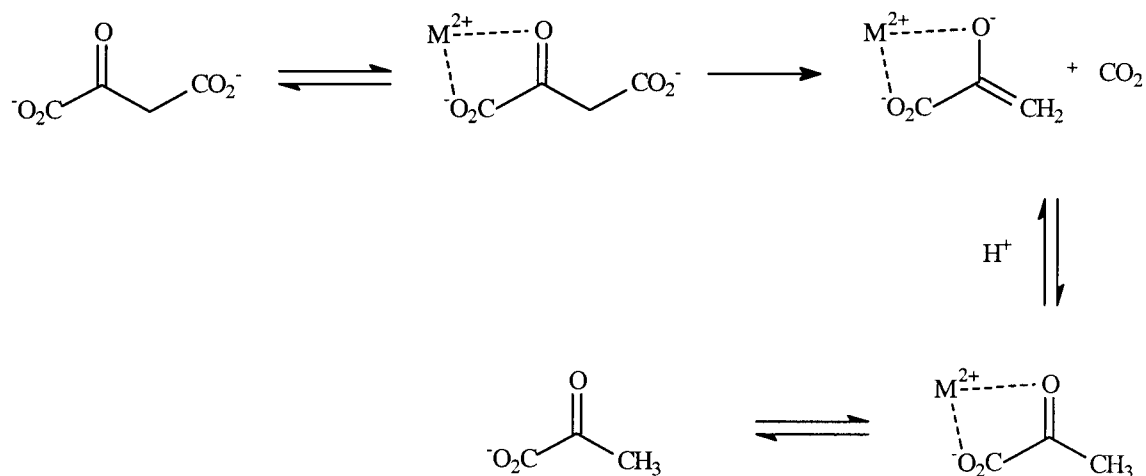
Scheme 4: Oxaloacetate decarboxylation mechanism.

Amino acid/pyridoxal (pyruvate) decarboxylations (Scheme 5) vary from both α-

keto acid/TPP and β-keto acid/metal ion decarboxylations because they contain no metal

ions. These types of decarboxylations generally use a cofactor known as pyridoxal-5'-

phosphate (PLP).[7-10] PLP-dependent processes initially occur by the covalent binding of

PLP to the enzyme via a Schiff base linkage to a lysine amino group. Non-covalent

interactions with the enzyme can also be seen with other PLP functional groups. Once

the substrate binds, it reacts to form a bound PLP-substrate Schiff base. The Schiff base

then loses CO_2 and forms a stabilized quinonoid intermediate, which is then reprotonated

with retention of configuration [11] and the amine is released.
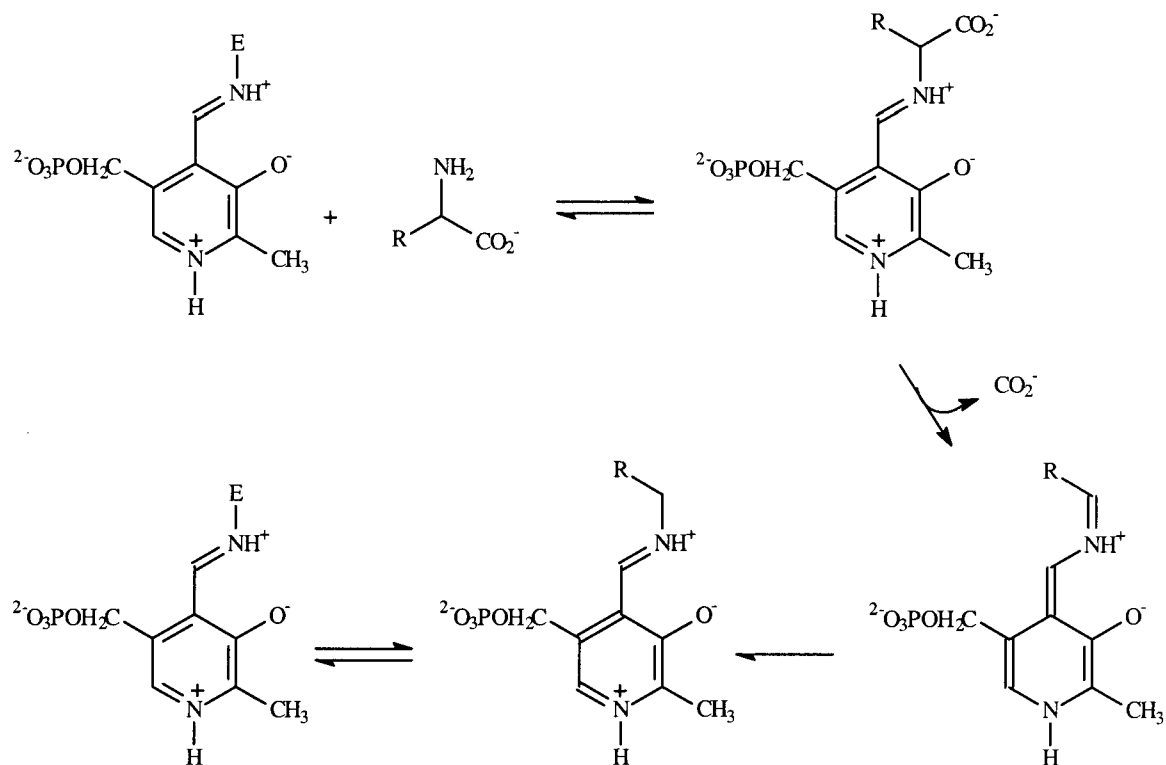
Scheme 5: PLP decarboxylation mechanism.

The final type of decarboxylation, the β-OH acid/oxidative decarboxylations

(Scheme 6) are similar to that of the β-keto acid/metal ion type except no metal ion is

involved in the mechanism. These enzymes, such as prephenate dehydrogenase, use a

cofactor, such as NAD^+ in order to abstract a hydride ion catalyzing the

decarboxylation.[12]
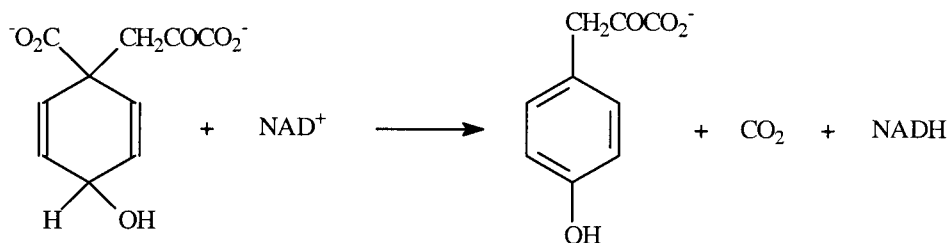
Scheme 6: Prephenate dehydrogenase.

The enzyme, orotidylate-5'-decarboxylase has been the subject of study by many enzymologists. As we know, ODCase is responsible for the decarboxyation of orotidine-5'-monophospate to uridine-5'-monophosphate in the final step of the *de novo* biosynthesis of pyrimidine nucleotides (Scheme 6), yet its catalytic mechanism is not understood. One characteristic that is not found in other decarboxylase is ODCase does not require either a cofactor or metal ion for catalysis. Various mechanistic hypotheses have been proposed to explain the process by which ODCase catalyzes decarboxylation.

Silverman and Groziak proposed an addition-elimination mechanism involving the formation of a covalently bound intermediate.[13] It was suggested that enzymatic decarboxylation proceeds through addition of a proton via an active site nucleophile at the C5/C6 double bond of OMP (Scheme 7).
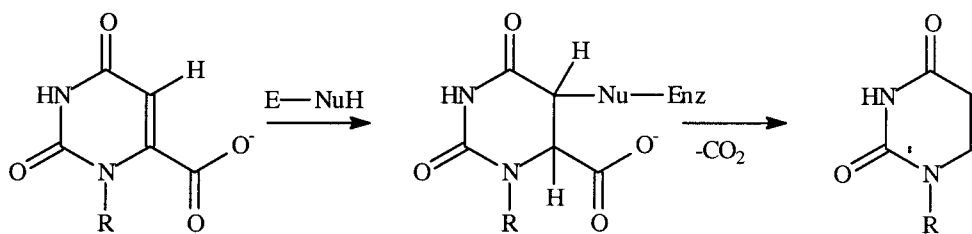
Scheme 7: Silverman and Groziak's proposed addition-elimination mechanism.

If nucleophilic addition were to occur at the C5 position, protonation would also occur at the C6 position. Reduction of the C5/C6 double bond would cause changes in the electron density around C5 and C6 that could be analyzed by NMR. The transition-state analogue 6-hydroxyUMP was used for this experiment. When the ^{13}C NMR analysis was performed no change was seen for the signals at C5 or C6.[14] Results of these experiments concluded that C5 undergoes little, if any change in geometry during the substrate's progress from the ground state to the transition-state for enzymatic decarboxylation.

Lee and Houk proposed a mechanism involving the protonation of OMP at the 4-oxygen position and formation of a stabilized carbene intermediate at C6 (Scheme 8).[15]
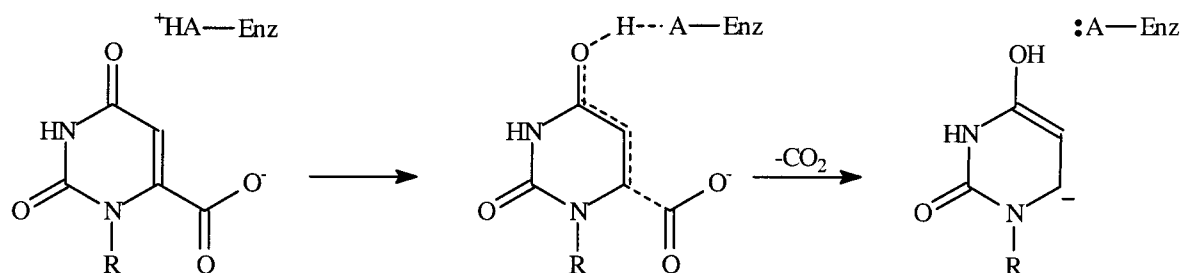
Scheme 8: Lee and Houk's 4-oxygen protonation mechanism

According to their quantum mechanical calculations, they predicted that the decarboxylation of 4-protonated orotate was more favorable then the decarboxylation of the 2-protonated orotate. The calculated enthalpy of activation for the decarboxylation of 4-protonated orotate was comparable with the enthalpy of activation determined later for this reaction.[16] Another reason that was presented to support their hypothesis was the fact that the 4-oxygen position in uracil is more basic than the 2-oxygen position.[17]

However, the crystal structures of OMP decarboxylase have revealed the absence of an

acidic residue near the 4-oxygen of a bound transition-state analogue and product, thus

reducing the possibility of a carbene-based mechanism. A revised version of the carbene-

based mechanism has been described that involves protonation of the 4-oxygen by a

water molecule, followed by formation of the stabilized carbene intermediate.[18]

Analysis via x-ray crystallography was performed by Appleby *et al.* [19] in order to

determine the decarboxylation mechanism of ODCase in *Bacillus subtilis* using UMP.

The authors proposed OMP decarboxylation proceeds by a bimolecular electrophilic

substitution mechanism (S_E2) in which decarboxylation and protonation are concerted.

According to the interpretation of crystallographic data, UMP binds in an orientation

within the enzyme where Lys62 (Lys93 in yeast ODCase) is found within proximity of

C6 in UMP. The authors concluded that the substrate OMP binds in a similar fashion

(Scheme 9).
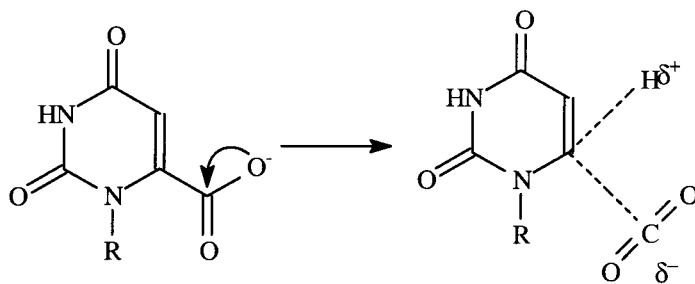
Scheme 9: Appleby *et al.* electrophilic substitution mechanism.

Beak and Siegel [20, 21] proposed a mechanism which involves the formation of a

nitrogen ylide intermediate (Scheme 10) which acts as an electron sink to aid the

breaking of the carbon-carbon bond. Ylide formation has been proposed to occur by the

protonation of the oxygen at C2 in the substrate with no covalent bond formed between the enzyme and substrate.
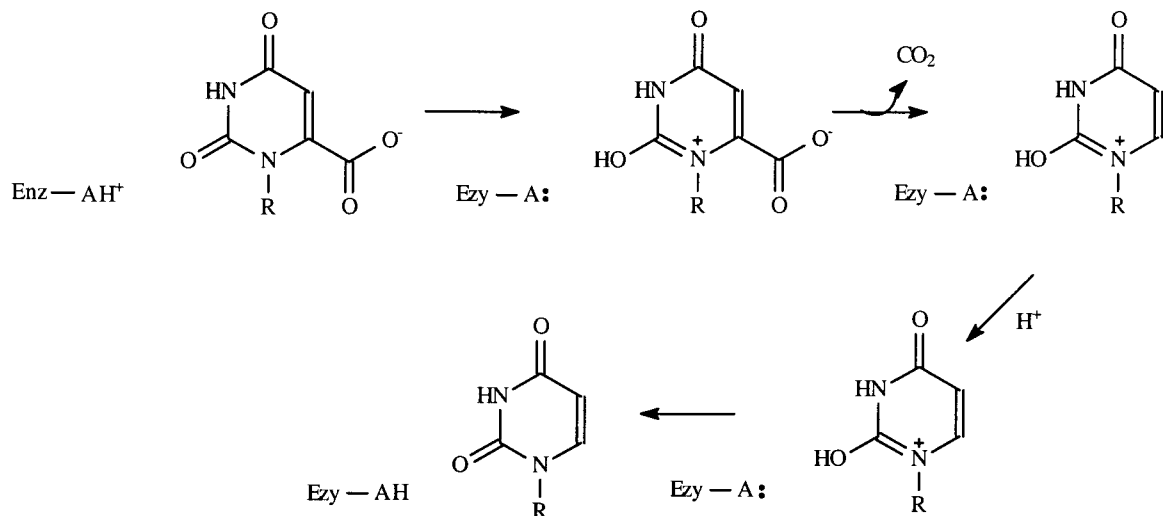
Scheme 10: Beak and Siegel's 2-oxygen protonation mechansim.

Transition-state analogue experiments by Levine *et al.* [22] presented 1-(5'-phospho-β-D-ribofuranosyl) barbituric acid (BMP) as a very tightly bound, reversible inhibitor of the yeast enzyme. Shostak and Jones performed studies using the analogue 5-azaOMP. The 5-azaOMP group is not electrophilic; therefore, an enzyme mechanism utilizing a nucleophilic addition of the enzyme at the C5 position can be ruled out.[23] They also performed spectral studies with 6-azauridylate (6-azaUMP), another ODCase inhibitor. Again, these studies provided evidence against the mechanism involving the loss of the C5 C6 double bond due to the fact that the UV absorption was maintained in the bound inhibitor. Acheson *et al.* also performed kinetic isotope effect studies on the

catalytic mechanism of ODCase. In these experiments, ODCase was titrated with ^{13}C-enriched BMP. ^{1}H-NMR studies showed only a small downfield displacement of the C5 resonance, indicating that no addition occurred at C5 of the inhibitor.[24]

This work [20-22, 24] has led our group to investigate further the ylide/zwitterion mechanism. This particular mechanism provides some interesting features that appear to be more favorable for both the enzyme and the bound substrate. Past studies of decarboxylase enzymes have shown how metals can act as cofactors in enzyme catalyzed decarboxylations. Miller *et al.* was able to prove that Zn^{2+} does exist within the yeast ODCase [25] however, its implications in catalysis have not yet been determined. In the ylide mechanism, the enzyme provides an environment in which the basicity of the substrate's 2-oxygen is increased so that the active site residues potentially could protonate the keto group. Smiley and Jones determined that Lys-93 plays a key catalytic role as a possible proton donor in yeast ODCase.[26]

It is our group's hypothesis that decarboxylation occurs via the ylide/zwitterion mechanism, as provided by Beak and Siegel.[20, 21] Through the use of various synthesized transition-state analogues, both isotopically labeled and unlabeled, we hope to provide information regarding the binding orientation of the substrate OMP using various spectroscopic studies.

Chapter 2: Synthesis of Transition-state Analogues

Introduction:

Transition-state analogues are stable molecules are chemically and structurally similar to the transition-state of the catalyzed reaction. These molecules tend to bind more with greater affinity than both the natural substrate and competitive inhibitors normally found in the presence of the enzyme.

Early studies, using the analogues 1-(5´-Phospho-β-D-ribofuranosyl) barbituric acid (BMP) and 6-Azauridine-5´-Phosphate (6-azaUMP) by Levine *et al.*, were used to investigate the uses of these analogues as transition-state inhibitors of ODCase. Further studies using the analogue 2-thio-orotidine-5´-monophosphate were performed in order to provide some insight on previous proposed catalytic mechanisms. [27] Ueda *et al.* studied the synthesis of a variety of 5-bromo derivatives of uridine-5´-monophosphate with subsequent synthesis of 6-cyano and 6-thiocarboxamido derivatives.[28]

The compound 6-thiocarboxamidouridine-5´-phosphate, a transition-state analogue, can be used to provide evidence on the catalytic decarboxylation mechanism of ODCase. Before spectroscopic techniques can begin, a modified version of the synthesis and purification of both 6-thiocarboxamidouridine-5´-phosphate by Ueda *et al.* and additional synthesis of ^{15}N enriched-6-thiocarboxamidouridine-5´-phosphate must be done. These modifications will be performed to enhance the purity and stability of synthesized analogues.

Materials:

Uridine-5′-monophosphate, sodium sulfate, pyridine, dimethylsulfoxide, dimethyformamide, and DOWEX 1x8-200 anion exchange resin were purchased from the Sigma Chemical Co. [15]N enriched sodium cyanide was purchased from Cambridge Isotope Laboratories.

Experimental:

5-Bromouridine-5′-Phosphate (2): Disodium salt of uridine-5′-monophosphate **1** (1.06 g, 2.87 mmol) was suspended in a mixture of 10.0 mL pyridine and 5.0 mL acetic acid. Bromine (2.29 g, 2.87 mmol) was added under stirring in an ice water bath and kept for 24 hours. The reaction was checked for completion via HPLC (Figure 1) then concentrated *in vacuo* yielding an orange anhydrous syrup which was redissolved in H_2O, and dried, several times and finally being dissolved in 10.0 mL H_2O with EtOH add to effect precipitation. The precipitate was collected by centrifugation and then redissolved in a minimal amount of H_2O. The crude **2** was applied to a column of DOWEX 1x8-200 anion exchange resin and washed with a linear gradient of H_2O (300 mL)/0.8M NH_4HCO_3 (300 mL) (0-100%). Fractions were checked for UV absorbance (λ_{max} 278 nm, λ_{min} 240 nm). Fractions containing 2 were concentrated yielding colorless crystals of **2** (0.99 g, 2.19 mmol).
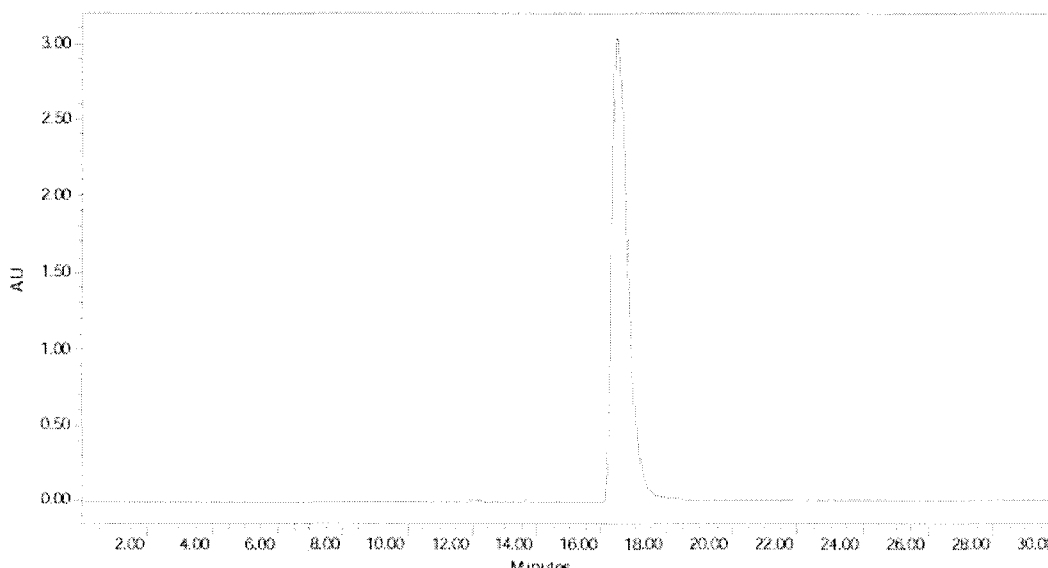
Figure 1: Ion exchange HPLC chromatogram of 5-Bromouridine-5′-Phosphate.

6-Cyanouridine-5′-Phosphate (3): Compound **2** (0.50 g, 1.09 mmol) was taken up

in 10.0 mL of dimethylformamide and evaporated to yield a syrup. The syrup was

dissolved in 17.0 mL dimethylsulfoxide and 0.141 g (2.18 mmol) NaCN was added and

stirred at room temperature for 48 h. To the reaction mixture 0.075 g (1.09 mmol) NaCN

was added in 3.0 mL dimethylsulfoxide and stirred at room temperature for 72 additional

h. The reaction was monitored for completion via HPLC (Figure 2), diluted with H_2O and

applied to a column of DOWEX 1x8-200 anion exchange resin and washed with a linear

gradient of H_2O (300 mL)/0.8 M NH_4HCO_3 (300 mL) (0-100%). Fractions were

collected, checked for UV absorbance (λ_{max} 279 nm, λ_{min} 238 nm). Fractions containing

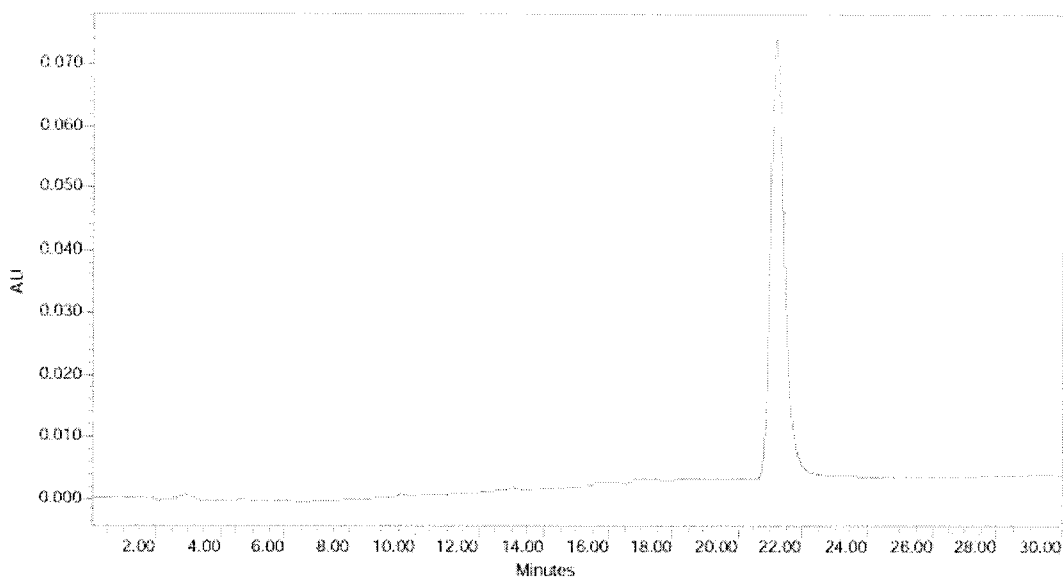**3** were collected and concentrated yielding an off-white powder.

Figure 2: Ion exchange HPLC chromatogram of 6-Cyanouridine-5'-Phosphate.

^{15}N enriched-6-Cyanouridine-5′-Phosphate (**4**): Compound **2** (0.50 g, 1.09 mmol) was taken up in 10.0 mL of dimethylformamide and evaporated to yield a syrup. This was dissolved in 17.0 mL dimethylsulfoxide and 0.141 g (2.18 mmol) ^{15}N enriched-NaCN was added and stirred at room temperature for 48 h. To the reaction mixture 0.075 g (1.09 mmol) ^{15}N enriched-NaCN was added in 3.0 mL dimethylsulfoxide and stirred at room temperature for 72 additional h. The reaction was monitored for completion via HPLC (Figure 3). Diluted with H_2O and applied to a column of DOWEX 1x8-200 anion exchange resin and washed with a linear gradient of H_2O (300 mL)/0.8 M NH_4HCO_3 (300 mL) (0-100%). Fractions were collected, checked for UV absorbance (λ_{max} 279 nm, λ_{min} 238 nm). Fractions containing **4** were collected and concentrated yielding an off-white powder.
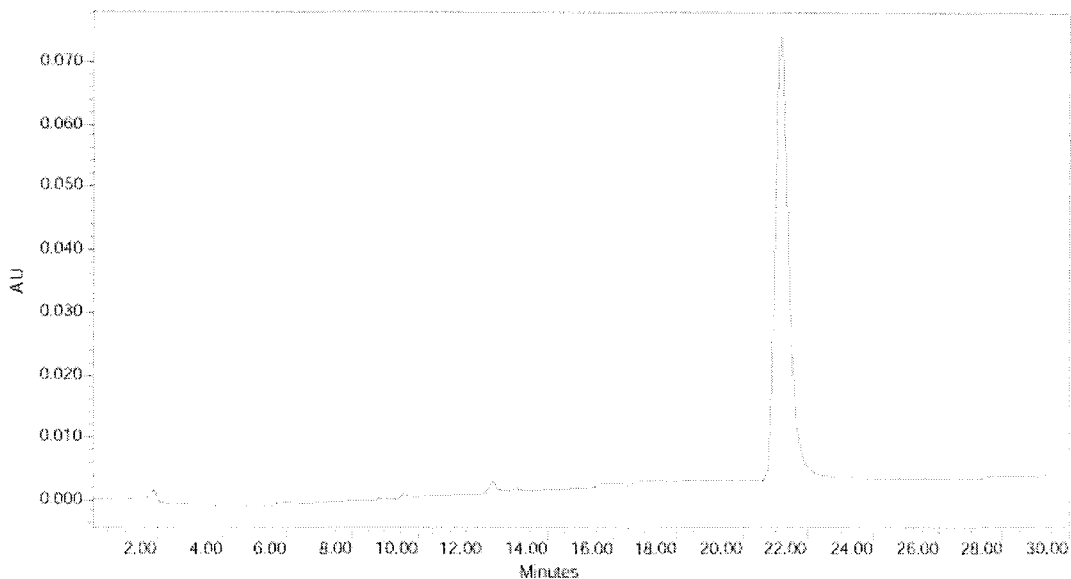
Figure 3: Ion exchange HPLC chromatogram of ^{15}N enriched 6-Cyanouridine-5′-Phosphate.

6-Thiocarboxamidouridine-5′-Phosphate (**5**): Ammonium salt of **3** was dissolved

in 30.0 mL of pyridine and H_2S gas was gently bubbled into the solution for 80 min.

After 80 min N_2 gas was bubbled to replace the H_2S. The reaction was monitored for

completion via HPLC (Figure 4), concentrated and redissolved in 10.0 mL H_2O and

applied to a column of DOWEX 1x8-200 anion exchange resin and washed with a linear

gradient of H_2O (300 mL)/0.8 M NH_4HCO_3 (300 mL) (0-100%). Fractions were collected,

checked for UV absorbance (λ_{max} 270 nm, λ_{min} 231 nm). Fractions containing **5** were

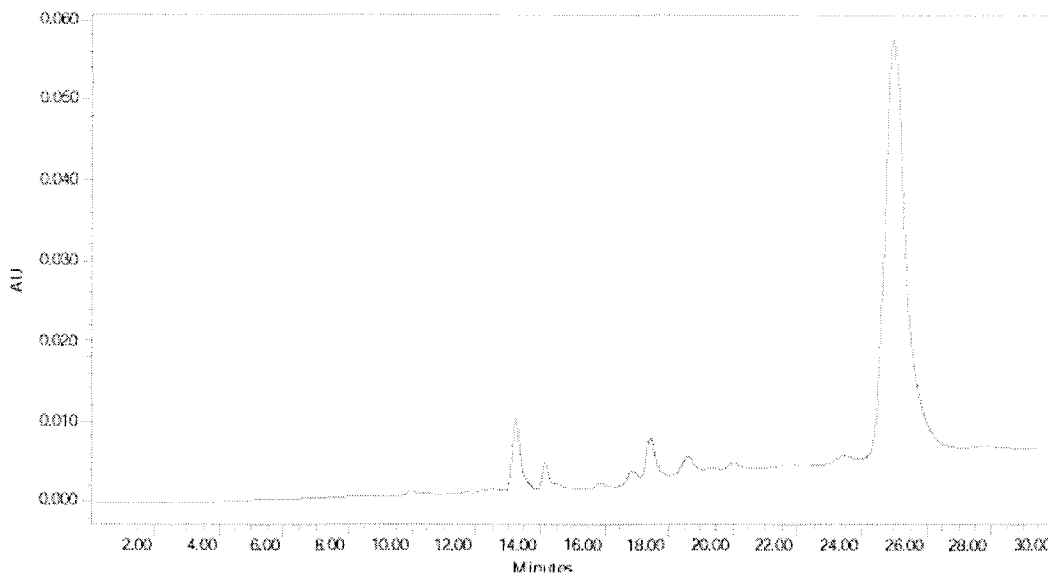collected and concentrated to 50.0 mL and stored at -20 °C.

Figure 4: Ion exchange HPLC chromatogram of 6-Thiocarboxamidouridine-5′-Phosphate.

[15]N enriched-6-Thiocarboxamidouridine-5′-Phosphate (**6**): Ammonium salt of **4** was dissolved in 30.0 mL of pyridine and H_2S gas gently bubbled into the solution for 80 min. After 80 min N_2 gas was bubbled to replace the H_2S. The reaction was monitored for completion via HPLC (Figure 5), concentrated and redissolved in 10.0 mL H_2O and applied to a column of DOWEX 1x8-200 anion exchange resin and washed with a linear gradient of H_2O (300 mL)/0.8 M NH_4HCO_3 (300 mL) (0-100%). Fractions were collected, checked for UV absorbance (λ_{max} 270 nm, λ_{min} 231 nm). Fractions containing **6** were collected and concentrated to 50.0 mL and stored at -20 °C.
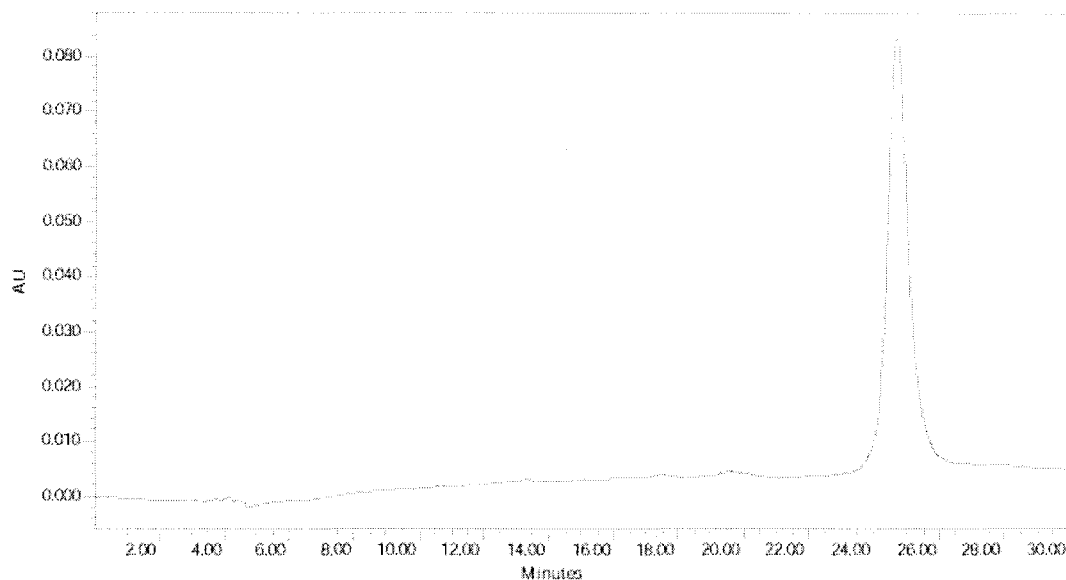
Figure 5: Ion exchange HPLC chromatogram of ^{15}N enriched 6-Thiocarboxamidouridine-5′-Phosphate.

Results and Discussion:

Synthesis of 5-bromouridine-5′-monophosphate was monitored via ion exchange HPLC chromatography. Figure 1 shows a lone peak representing **2** elutes at 17min showing complete conversion and purification of **1** to **2**. UV absorbance, λ_{max} 278 nm, λ_{min} 240 nm, was used to confirm the identity of **2** as reported by Ueda *et al.*

Analysis of the synthesis and purification of both the ^{15}N-enriched and unlabeled 6-cyanouridine-5′-monophosphate was monitored using ion exchange HPLC chromatography. HPLC spectra once again show the complete conversion of **2** to **3** (Figure 2) and **2** to **4** (Figure 3) with a lone peak at approximately 21 min. UV absorbance of **3** λ_{max} 279 nm, λ_{min} 238 nm and **4** λ_{max} 279 nm, λ_{min} 238 nm were compared to reported values of Ueda *et al.* to confirm product identities.

Synthesis and purification of both the ^{15}N-enriched and unlabeled 6-thiocarboxamidouridine-5′-phosphate was monitored using ion exchange HPLC chromatography. Chromatograms reveal the synthesis of **5** (Figure 4) and **6** (Figure 5) with the most intense peak found at 25 min. UV absorbance of **5** λ_{max} 270 nm, λ_{min} 231 nm and **6** λ_{max} 270 nm, λ_{min} 231 nm were compared to reported values of Ueda *et al.* LC-MS data was also reported for both **5** (Figure 6) and **6** (Figure 7).

X-ray crystallographers have resolved structures of the ODCase/UMP complex where C6 of the pyrimidine ring lies facing Lys-93 (Figure 8).[19] From this data it has been proposed that OMP binds in a similar fashion (Figure 8). However, it has been
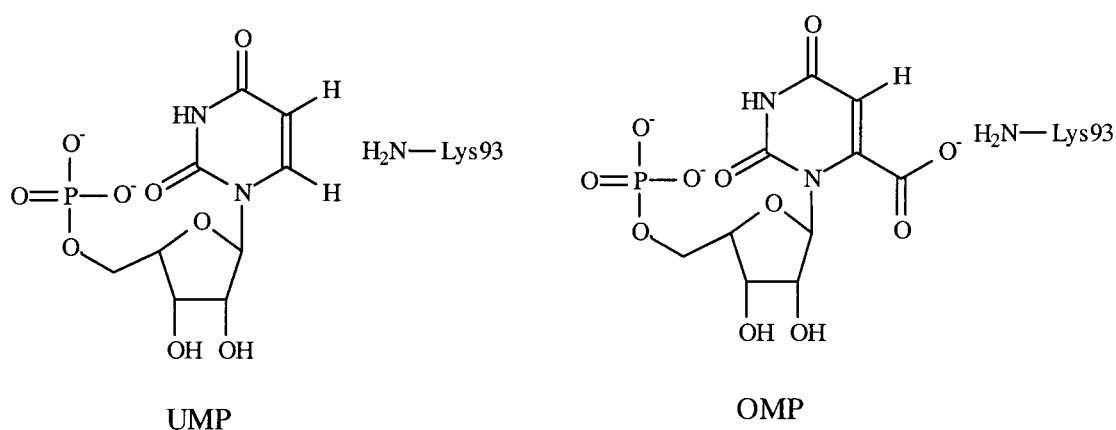

Figure 8: Proposed binding scheme of UMP and OMP from x-ray crystal structures.

proposed [20, 21] that OMP binds in a reverse orientation in the enzyme active site where O2 and not C6 faces Lys-93 (Figure 9).

Ramen spectroscopic studies can be performed using 6-thiocarboxamidouridine-5′-monophosphate to provide evidence of a binding scheme in ODCase where O2 is

found facing Lys-93. If protonation were to occur at O2 a "stretch" in the C2-O2 bond would be observed.

The analogue, ^{15}N-enriched 6-thiocarboxamidouridine-5′-phosphate, would allow us to observe any intramolecular ^{31}P-^{15}N and ^{31}P-^{1}H scalar couplings across hydrogen bonds. Such a coupling was reported with human Ras p21 Q61L protein complexed with GDP.[33] If the binding orientation of the analogue were in such a position that O-2 faced Lys-93, a possible coupling could be observed with the phosphate group of the ribose phosphate and protons adjacent to ^{15}N enriched thiocarboxamido substituent of the pyrimidine ring. A current analysis of this coupling is under way at Penn State University by the Lecomte Group.
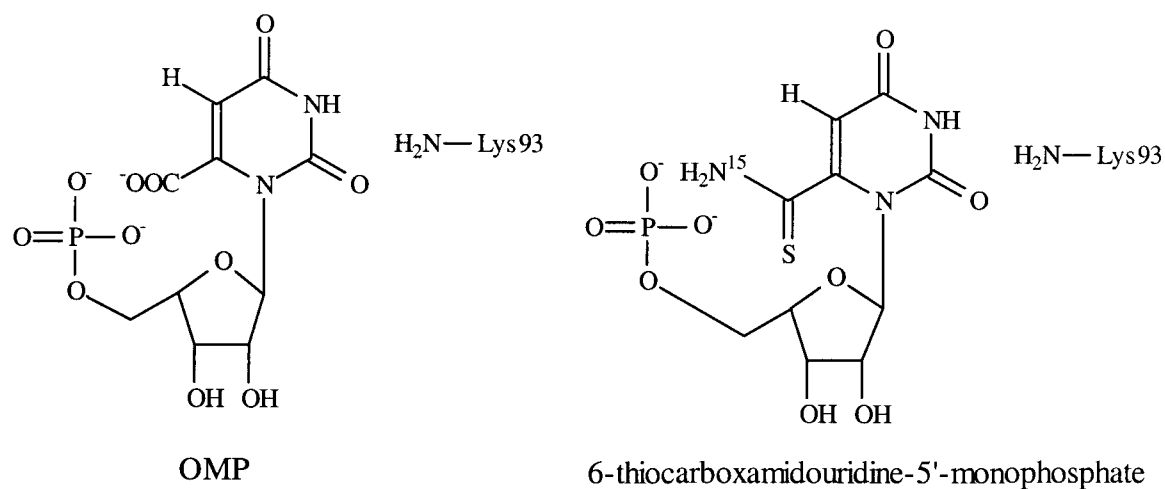

Figure 9: Proposed binding scheme of OMP (left) and 6-thiocarboxamidouridine-5′-phosphate in the proposed ylide/zwitterion mechanism.
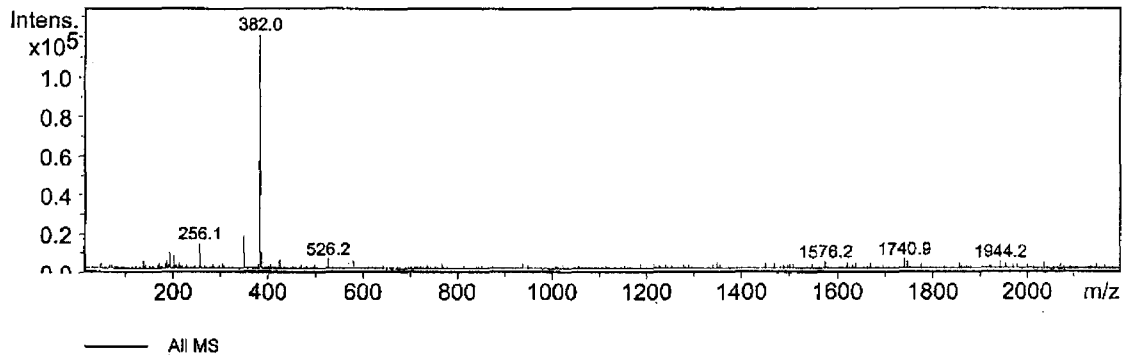
Figure 7: EI-MS of ^{15}N-enriched 6-thiocarboxamidouridine-5′-phosphate (negative

mode).

Chapter 3: Yeast ODCase Purification and Spectroscopic Analysis with 6-thiocarboxamidouridine-5'-phosphate

Introduction:

In order to perform any spectroscopic analysis techniques, pure ODCase was prepared from yeast strain BJ5424 transformed with the plasmid pGU2. This plasmid contains the gene *ura3* for ODCase.[29] Yeast cultures were grown, induced with galactose followed by cell lysis. Initial ODCase purification was done via ammonium sulfate fractionation (60%-90%) followed by a series of column purifications, including Affi-Gel Blue affinity chromatography [30] and ion exchange column chromatography. Protein purity was monitored using SDS-polyacrylamide gel electrophoresis.

Once purified ODCase was obtained, ^{1}H NMR analysis can be performed on the protein and protein + ligand to not only confirm binding of the ligand but also determine whether or not the protein maintains quaternary structure.

Materials:

Yeast extract, peptone, agar, glucose, galactose, sucrose were from Fisher Biotech. Phenylmethylsulfonyl fluoride (PMSF), pepstatin A, leupeptin and BSA were purchased from Sigma. Yeast nitrogen base without amino acids was from Difco. Affi-Gel Blue and Bradford reagent were purchased from Bio-rad. Glycerol, TEMED and ammonium sulfate were from Amresco. Yeast strain BJ5424 was from the Yeast Genetic Stock Center, University of California, Berkeley.

SDS-Polyacrylamide Gel Electrophoresis:

Electrophoresis separates biological molecules based on their charge and
frictional coefficient. In polyacrylamide gel electrophoresis (PAGE), gels are made by
the polymerization of polyacrylamide that is induced by ammonium persulfate (APS) and
tetramethylethylenediamine (TEMED). Sodium dodecyl sulfate (SDS) is a detergent that
denatures proteins and causes them to assume a rod-like shape. All SDS-treated proteins
have identical charge-to-mass ratios and similar shapes. Therefore, in SDS-PAGE
proteins will be separated based on their molecular weights, where those with lower
molecular weights will migrate further down the length of the gel.[31]

Bradford Assay:

A Bradford assay is used to determine protein concentrations of various samples
using a standard bovine serum albumin (BSA) and a dye known as Coomassie brilliant
blue G-250. When protein binds to the coomassie dye, a shift in the absorbance occurs
from λ_{max} = 465nm to λ_{max} = 595nm. All absorbance readings were taken using a
Hewlett Packard 8452 diode array spectrophotometer.

Affinity Chromatography:

Affinity chromatography is a method that allows for the purification and isolation
of various biomolecules including enzymes, antibodies, antigens, nucleic acids, proteins
and other biochemical materials.[31] Its function is to bind specific biological molecules
using selective ligands covalently bound to an agarose resin. Molecules of interest can
then be eluted by changing the ionic strength, pH, or by adding a competing ligand.

Affinity chromatography is used for the purification of yeast ODCase. Affi-Gel blue is a beaded, cross-linked agarose gel with covalently attached Cibacron Blue F3GA dye. Upon ODCase binding a buffer containing one of variety of weak inhibitors, such as 6-azaUMP, can be applied to the column. Application of this second ligand allows the elution of the ODCase protein from the blue dye.

Ion Exchange Chromatography:

Proteins have a wide variety of distinguishing characteristics, including ionic strength. This characteristic allows their purification by ion exchange chromatography. In this process a stable resin bead possesses one of two different possible ionic charges, either positive (cation) or negative (anion). The net ionic charge of the protein can be used to help determine which form of the column resin is to be used. Positively charged proteins will bind to anionic resins while negatively charged proteins will bind to cationic exchange resins. Once the protein is bound to the column, various buffers, varying in pH or salt concentration, can be used to affect the binding affinity of the protein. Protein elution can be performed by applying buffers with varying salt concentrations. At low salt concentrations, weak affinity proteins elute from the column while stronger binding proteins remain. Only by increasing salt concentration can one then elute proteins with a stronger binding affinity and, therefore, proteins of interest.

Yeast Growth Protocol:

The transformed yeast cells with pGU2 plasmid were selected according to their ability to grow on synthetic complete medium agar plate containing 2% (w/w) glucose in

the absence of leucine (Leu) and uracil. Synthetic complete medium (SCM) consists of 0.13 g/L dropout powder containing: 4% adenine, tryptophan, histidine, arginine and methionine; 6% tyrosine, lysine, and isoleucine/ 10% phenylalanine and valine and 40% threonine,[29] 0.17 g/L yeast nitrogen base without amino acids, 0.5 g/L ammonium sulfate, all dissolved in 90 mL of water and adjusted to pH 6.0. SCM agar is prepared by the addition of 1.5 g agar to the above SCM medium.

Colonies appeared in 4-5 days and were then selected from the SCM/agar plates and transferred into test tubes containing 9 mL/1 mL YP/glucose media. Inoculated test tubes were incubated at 30°C with shaking for 48 hrs using a Fisher Isotemp incubator model 2550. YP/glucose was prepared containing 1.0 g yeast extract, 2.0 g peptone dissolved in 90 mL of water. Once autoclaved, 10 mL of 20% (w/v) sterile glucose was added. 3.0 mL of yeast cells were transferred from YP/glucose cultures to SCM/sucrose (81.0mL SCM/9.0mL 20% w/v sucrose) media and incubated at 30°C with shaking for 16hrs. Following incubation, 20 mL of the SCM/sucrose culture was transferred into each of four 900 mL flasks of YP medium consisting of 11.0 g yeast extract, 18.0 g peptone dissolved in 810 mL of water. 90 mL of 20% (w/v) sterile sucrose was added and the flasks were incubated at 30°C with shaking for 12 hrs. Upon reaching the 12 hr. incubation time, 100 mL of 20% (w/v) sterile galactose was added and incubation was continued for 9-10 hrs. Yeast cells were collected by centrifugation and then lysed.

Purification of Yeast ODCase:

Yeast ODCase was obtained from the organism *Saccharomyces cerevisae* strain BJ5424 transformed with the plasmid pGU2, which carries the *ura3* gene for ODCase.

Cells, once grown via the yeast growth protocol, were harvested in pre-weighed bottles at

8000 rpm for 10 min. at 4°C in a Sorvall RC 5B Plus. The weighed pellets were re-

suspended in 50mM potassium phosphate buffer (pH 7.5) containing 10% (v/v) glycerol,

5 mM β-mercaptoethanol, 1 mM PMSF, 2 μM pepstatin and 0.6 μM (lysis buffer).

Lysis was done using a Bead Beater (Biospec Products): 5x at 60-sec intervals with 120-

sec periods in between each pulse to allow cooling of the protein. Centrifugation was

performed at 13,000 rpm for 20 min. in order to remove cell debris. The supernatant

volume was measured and fractionated from 60%-90% using solid ammonium sulfate.

The pellet from the 90% ammonium sulfate fractionation was then re-dissolved with lysis

buffer (15 mL) and dialyzed against 1.0 L 50 mM Tris buffer (pH 7.0) containing 10%

(v/v) glycerol and 5 mM β-mercaptoethanol (column/dialysis buffer) for 18 hrs. at 4°C

followed by 2 additional 1-2 hr dialysis at 4°C in order to remove ammonium sulfate salts.

The dialyzed, crude protein solution was then applied to an Affi-Gel Blue column

at a flow rate of 3.0 mL/min. The column was run using column/dialysis buffers at 3.0

mL/min. Non-specific binding proteins passed over the column and were removed.

Qualitative analysis of fractions was performed using prepared Bradford protein reagent.

Once all non-specific binding proteins were removed, ODCase was eluted using

column/dialysis buffer containing 50mM 6-azaUMP at a flow rate of 3.0 mL/min.

ODCase elution was monitored, qualitatively, using Bradford protein reagent. Upon

complete elution of ODCase, the column was washed using 400-mL column/dialysis

buffer containing 200 mM NaCl followed by equilibrating the column with 500 mL of

column/dialysis buffer. Fractions containing ODCase were collected and concentrated to

approximately 10 mL (10 mg/mL) using an Amicon Stirred Cell Ultrafiltration apparatus

and Diaflow Ultrafiltration membrane. Protein concentration was monitored via Bradford assay. SDS-PAGE gel electrophoresis (lanes 2 and 3) was carried out on 12% gels in order to confirm ODCase purification with a band consistent with the molecular weight of ODCase at 29,500 Da (Figure 10). A faint thin band of protein slightly heavier then ODCase can also be seen. The semi-purified protein was then stored at 4°C until further purification was performed.

Further purification of ODCase was performed via ion-exchange column chromatography. A column was prepared (1.5 x 50 cm) using DEAE Sepharose resin in order to remove a small protein band at approximately 40,000 daltons along with excess 6-azaUMP from the previous column purification. The column was first washed with 200 mL of column/dialysis buffer containing 200 mM NaCl at 3.0 mL/min. to remove any unwanted contaminants. The column was equilibrated with 400 mL of HEPES column/dialysis (50 mM HEPES instead of Tris) buffer. Protein aliquots were applied to the column with HEPES column/dialysis buffer used to remove all the ODCase from the column. Protein fractions were, again, monitored qualitatively using Bradford reagent for ODCase. Fractions containing ODCase appeared first and were combined and concentrated to 5.0 mg/mL using an Amicon Stirred Cell Ultrafiltration apparatus and Diaflow Ultrafiltration membrane. Analysis via SDS-polyacrylamide gel, lanes 4 and 5 (Figure 10) shows a single band at approximately 29,500 daltons which is, again, in agreement with the molecular weight of 29,500 daltons. Pure protein was then stored at 4°C for future analysis.
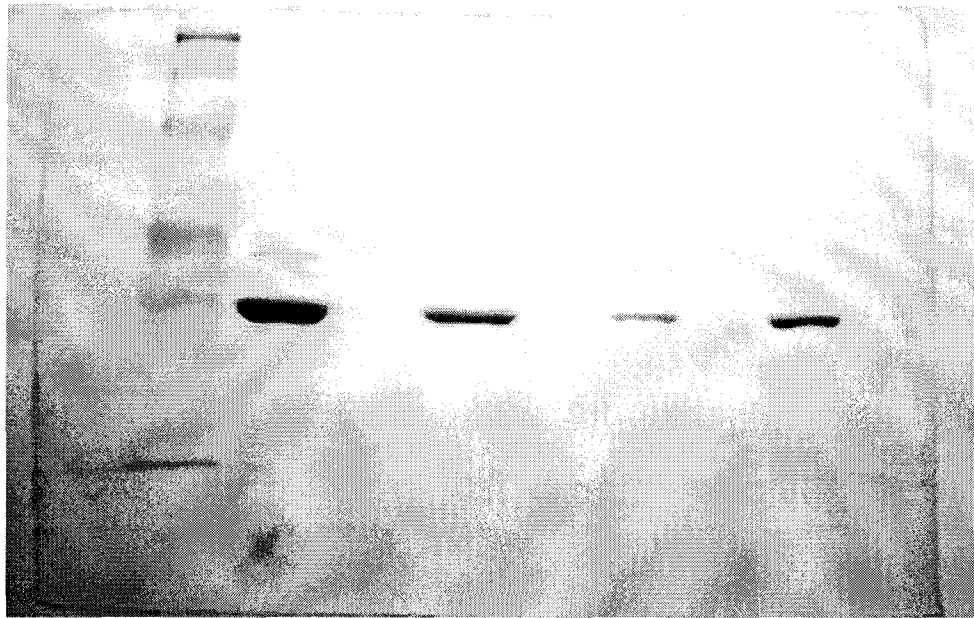
Figure 10: 12% SDS-PAGE gel; Protein molecular wt. marker (lane 2), affinity column purified ODCase (lane 3/5) and ion exchange column purified ODCase (lane 7/9).

Results and Discussion:

The resulting SDS-PAGE gel (Figure 10) shows that further purification of ODCase can be achieved using the DEAE Sepharous column (gel lanes 4 and 5) after purification with the Affi-Gel Blue affinity column (gel lanes 2 and 3).

Analysis of ^{1}H NMR for both ODCase (Figure 11) vs. ODCase/6-thiocarboxamidouridine-5'-phosphate complex (Figure 12) shows the appearance of a new signal at 12.3 ppm. Since no H signal exists for either ODCase or 6-thiocarboxamidouridine-5'-phosphate at this particular ppm, it has been concluded that this new signal is due to the interaction between ODCase and 6-thiocarboxamidouridine-5'-phosphate.

Figure 11: ^{1}H NMR of ODCase.

xx031203r 1
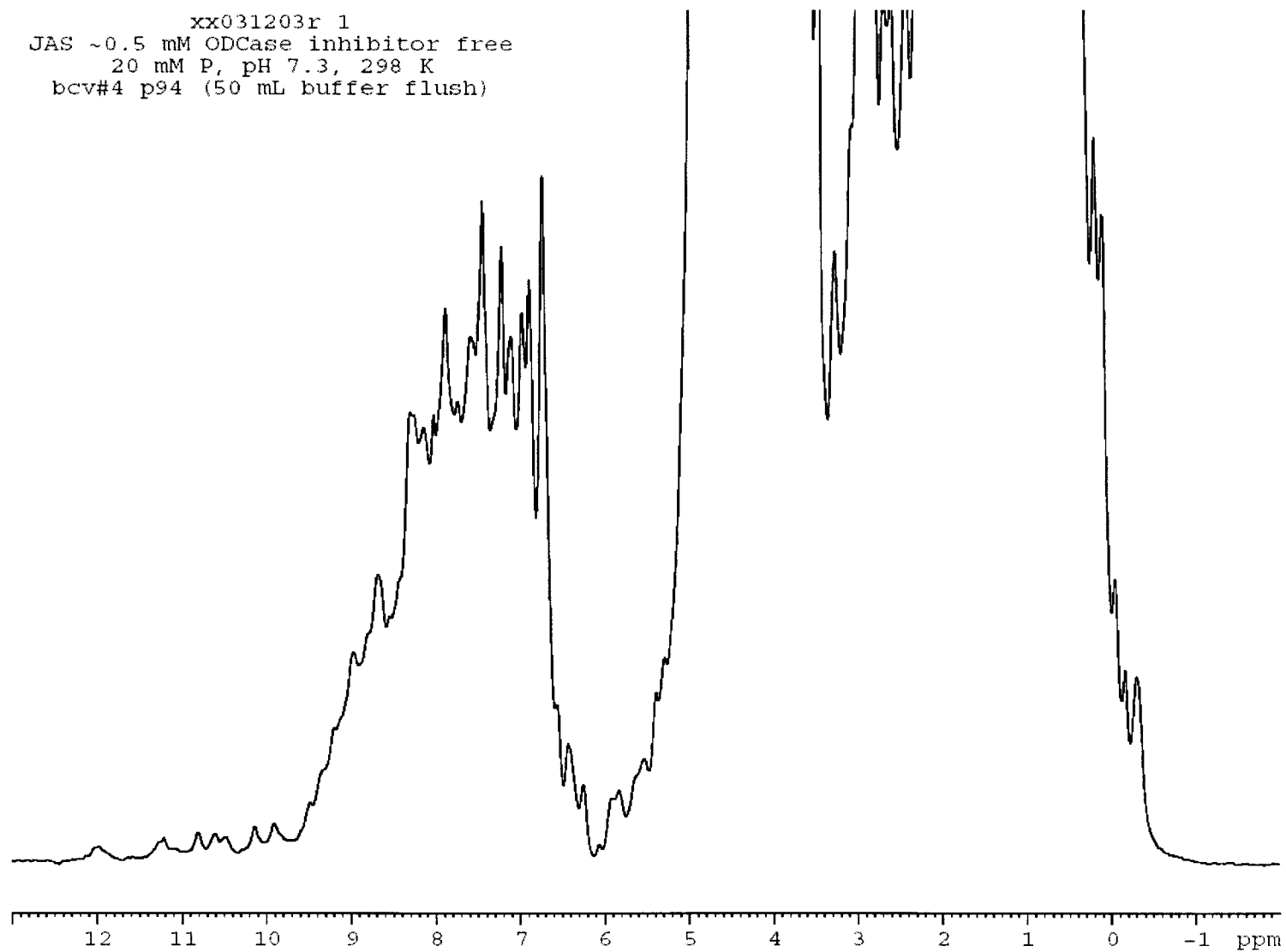JAS ~0.5 mM ODCase inhibitor free
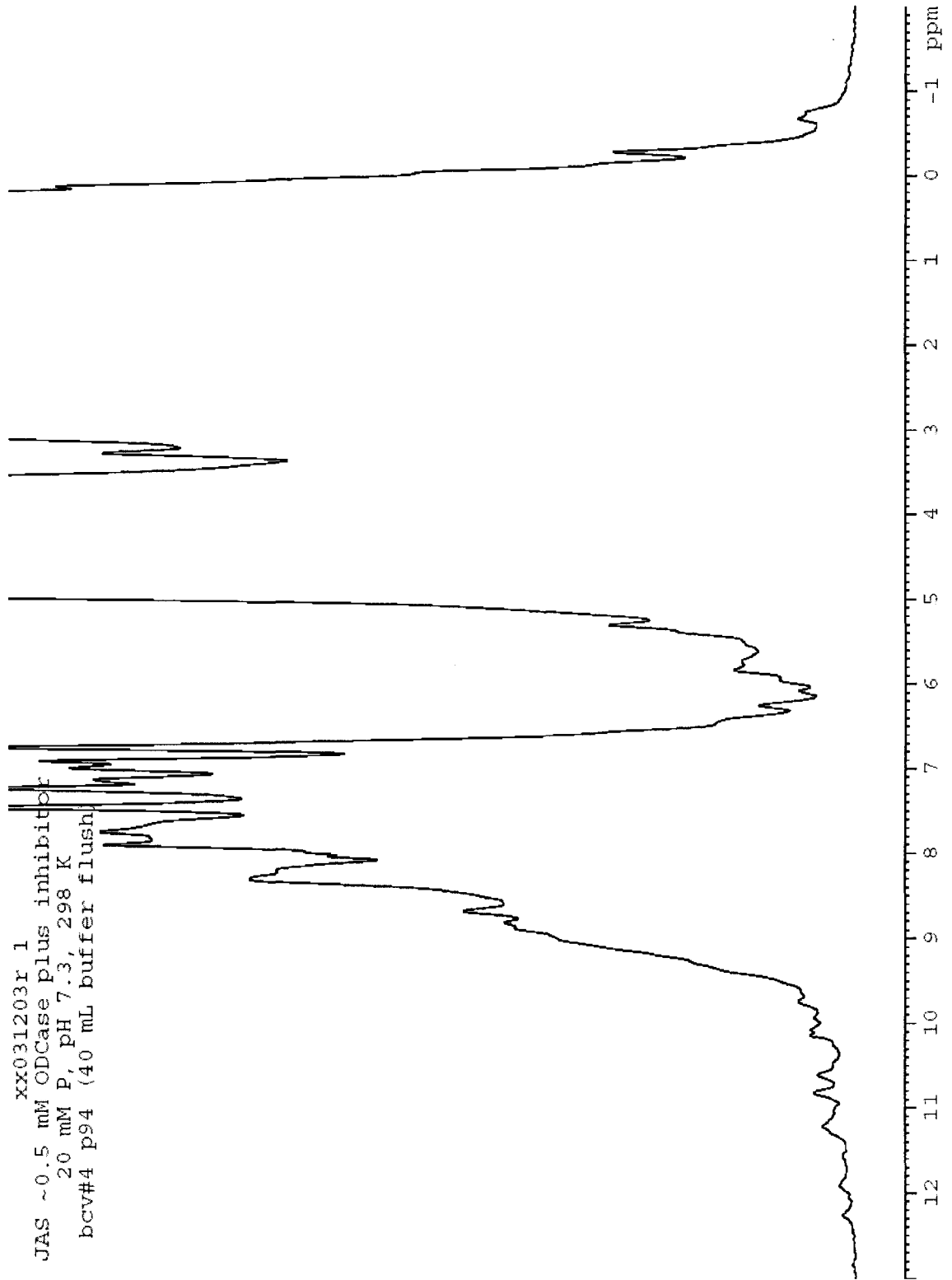20 mM P, pH 7.3, 298 K
bcv#4 p94 (50 mL buffer flush)

Figure 12: ^{1}H NMR of ODCase/6-thioamidouridine-5'-monophosphate complex.

# Chapter 4: Hydrogen Isotope Tracing in OMP Decarboxylase

Introduction:

The catalytic mechanism of the enzyme orotidine-5'-monophosphate

decarboxylase has not yet been fully characterized. Various mechanisms have been

proposed [13, 15, 18, 20-21], some of which suggest the possibility of hydrogen rearrangement

from C5 to C6 of the pyrimidine ring or the loss of H5 to solvent during catalysis.

Previous work by Creasy and Handschumacher [32] reported only 70% of the ^3H label were

lost from the resulting UMP, which was attributed to an incomplete ^3H release reaction.

Loss of the ^3H label could be the result of a transfer from C5 to another site found within

the molecule, which could provide some clues as to the catalytic mechanism.

The proposed O2 protonation mechanism (Scheme 10) may involve a

rearrangement of the decarboxylated intermediates. If a hydrogen shift from C5 to C6

were to occur, it would account for the results reported by Creasey and Handschumer [32]

and would provide strong evidence in support of a reaction involving a decarboxylated

intermediate capable of rearrangement as seen in (Scheme 10).

The electrophilic substitution mechanism proposed by Appleby et al. (Scheme 9)

does not suggest any reaction that could result in the loss to solvent or rearrangement of

H5. Therefore, any observed hydrogen shift involving H5 would provide evidence

against this mechanism. However, Silverman and Groziak's proposed addition-

elimination mechanism (Scheme 7) must undergo rearrangement to achieve the final

product UMP. If the reaction were enzymatically directed, the hydrogen at C5 in OMP

would also be found in the product UMP. However, if the rearrangement were not

enzymatically directed, the amount of deuterium isotope at C5 of OMP would be diminished in the product UMP.

In this experiment, the synthesis of [5-^{2}H] orotidine-5'-monophosphate will be carried out in order to observe any possible rearrangement that may occur during the enzymatic decarboxylation to [5-^{2}H] uridine-5'-monophosphate (Scheme 11).
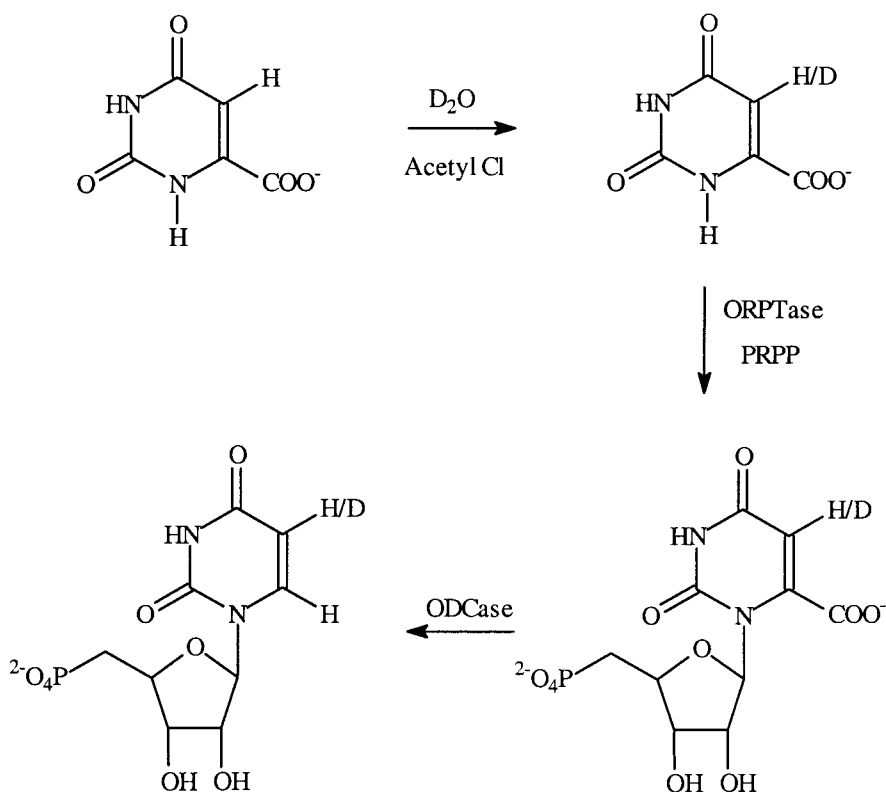
Scheme 11: Enzymatic synthesis of [5-^{2}H] uridine-5'-monophosphate.

Materials:

Orotic acid and 5-phosphoribosyl-1-pyrophosphate (PRPP) were purchased from the Sigma Chemical Co. Deuterium oxide (D_2O) and deuterated dimethyl sulfoxide were

purchased from Cambridge Isotope Laboratories. The laboratory of Dr. Charles

Grubmeyer, Temple University provided the enzyme orotate phosphoribosyltransferase.

All ^{1}H NMR were taken with a Varian Gemini 2000 400-MHz NMR spectrophotometer.

Experimental:

[5-^{2}H] Orotic acid (2): Orotic acid **1** (300 mg, 1.72 mmol) was dissolved in 15.0

mL deuterium oxide. 22.5 mL acetyl chloride was added drop wise under stirring in an

ice bath and kept under reflux for 96 h. While hot, the reaction mixture was filtered and

recrystallized 3x with boiling H_2O. Once recrystallization was complete the reaction was

washed with cold H_2O and concentrated in vacuo yielding an off-white powder. ^{1}H NMR

(Figure 13) was performed to characterize the product.

[5-^{2}H] Orotidine-5'-Monophosphate (3): Compound **2** (20.0 mg, 0.115 mmol)

was dissolved in a mixture of 19.8 mL H_2O, 1.8 mL Tris buffer, 67.5 µL MgCl$_2$, 112.5

µg PRPP, 180 µL OPRtase, 90 µL PPtase. The mixture was incubated at 30°C for 3 h

and monitored via HPLC for completion. Compound **3** was applied to a column of

Dowex Anion Exchange Resin. The column was washed with a gradient (0-100%) of

H_2O/NH$_4$HCO$_3$ and fractions collected and monitored via UV-absorbance (280nm).

Fractions were collected and concentrated *in vacuo* yielding an off-white powder. ^{1}H

NMR (Figure 14) was performed to characterize the product.

[5-^{2}H] Uridine-5'-Monophosphate (4): Compound **3** (10.0 mg, 0.0574 mmol) was

dissolved in a mixture of 10.0 mL H_2O, 2.0 µL ODCase (1.0 mmol). The mixture was

incubated at 30 °C for 3 h and monitored via HPLC for completion. Compound **4** was applied to a column of Dowex Anion Exchange Resin. The column was washed with a gradient (0-100%) of H_2O/NH_4HCO_3 and fractions collected and monitored via UV-absorbance (280nm). Fractions were collected and concentrated *in vacuo* yielding an off-white powder. ^1H NMR (Figure 15) was performed to characterize product.

Results and Discussion:

The analysis of ^1H NMR signals for **3** and **4** are complex due to the fact that signals for H5 and H1' both yield proton signals at 5.8 ppm. This overlap in signals, however, does not prevent us from determining the ratio, $^1H/^2H$, at C5 and C6 of UMP. A comparison of ^1H NMR for **2** and **3** (Figure13 and 14) calculated only 72% deuteration at the C5 position. This partially deuterated OMP, however, can be used for the analysis of a possible hydrogen shift from C5 to C6 in the ODCase reaction.

Initial analysis of ^1H NMR shows ODCase does not catalyze hydrogen exchange of UMP to an extent detectable under our experimental conditions. Figures 13 and 14 show the ^1H NMR spectrum of signals from UMP H6, H5 and H1' both before and after the addition of ODCase. The integral ratio of these signals, 1:1.8, does not change between either spectrum during catalysis. The presence of singlets for the H5 or H6 signals cannot be found. Signals such as these would indicate deuterium substitution at their respective neighboring positions.

Further analysis shows 100% retention of H at the C5 position during ODCase catalysis. This is achieved by first developing a measured integral ratio in the UMP product, H6/(H6+H5+H1'), which was found to be 0.44 for this experiment. The

equation $\{f_R + [(1 - f_R) \times f_H]\}/(2 + f_H)$ allows us to determine the % retention of H at C5. f_H

is a function of the fraction of ^{1}H in the partially deuterated OMP. The term f_R represents

the amount of ^{1}H arising at H6 from solvent in that the fraction of retention where $f_R =$

1.0 indicates no hydrogen shift and $f_R = 0.0$ indicates 100% hydrogen shift during

catalysis. $[(1 - f_R) \times f_H]$ describes the relative amount of ^{1}H arising from ^{1}H$_2$O solvent.

Algebraic rearrangement of the equation $\{f_R + [(1 - f_R) \times f_H]\}/(2 + f_H)$ to $[(1 - f_H) / (2 + f_H)]$

$\times f_R + f_H / (2 + f_H)$ gives a linear representation of the equation and a plot of the measured

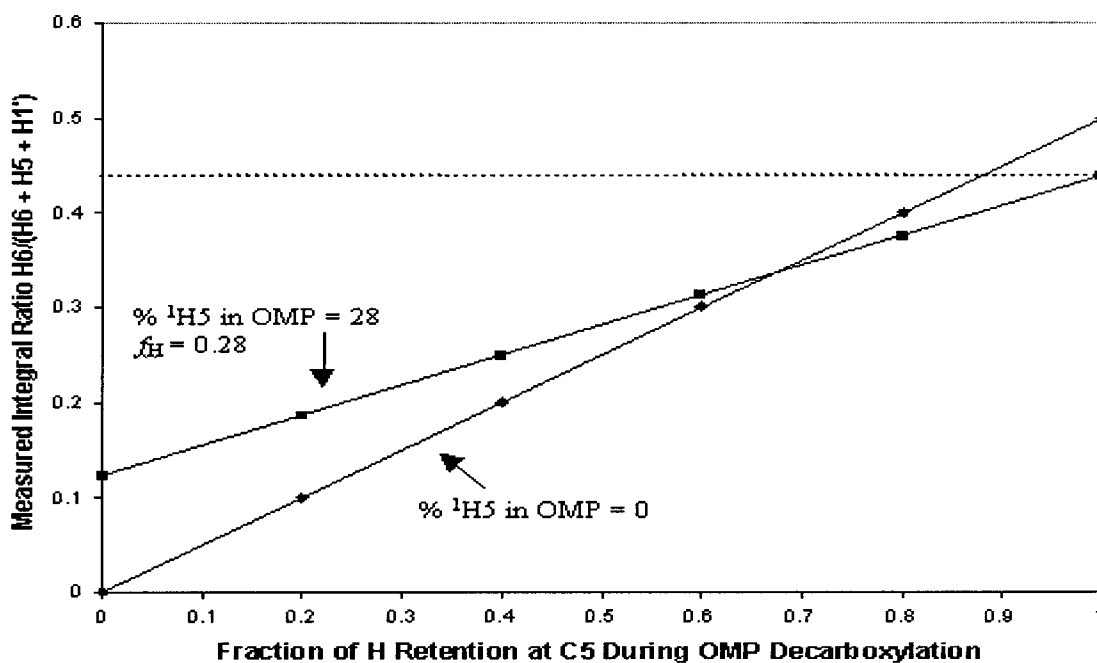intergral ratio vs. $[(1 - f_H) / (2 + f_H)] \times f_R + f_H / (2 + f_H)$ can be generated (Figure 16)

Figure 16: Graph showing the relationship of ^{1}H NMR integral ratios of the signals
corresponding to H6, H5 and H1' in partially deuterated UMP resulting from the
decarboxylation of partially deuterated OMP and the degree of hydrogen retention that
must be present in the ODCase reaction to yield the respective integral ratios.

Figure 16 illustrates the relationship between a measured UMP ^{1}H NMR integral

ratio H6/(H6+H5+H1') and the degree of hydrogen shift that must occur to yield the

measured UMP integral ratio, when the OMP used in the decarboxylation reaction is

deuterated to different extents. The first slope generated represents 100% deuteration of

OMP or $f_H = 0$ while the second slope generated represents our experimental results of

72% deuteration or $f_H = 0.28$ as seen on the graph. The horizontal line seen on the graph

represents the measured integral ratio of UMP as described above.

According to our results we can conclude that the hydrogen at the C5 position is

retained in its entirety at C5 in the decarboxylated product for two reasons. The first,

Figure 16, shows 100% retention at C5, which is observed using the plot of 72%,

deuterated OMP. Second the ^{1}H NMR signal (Figure 15) for H5 is found to be a doublet.

A deuterium shift from C5 to C6 during decarboxylation would have resulted in

formation of a singlet (representing ^{1}H5-^{2}H6-OMP) found between the two peaks of the

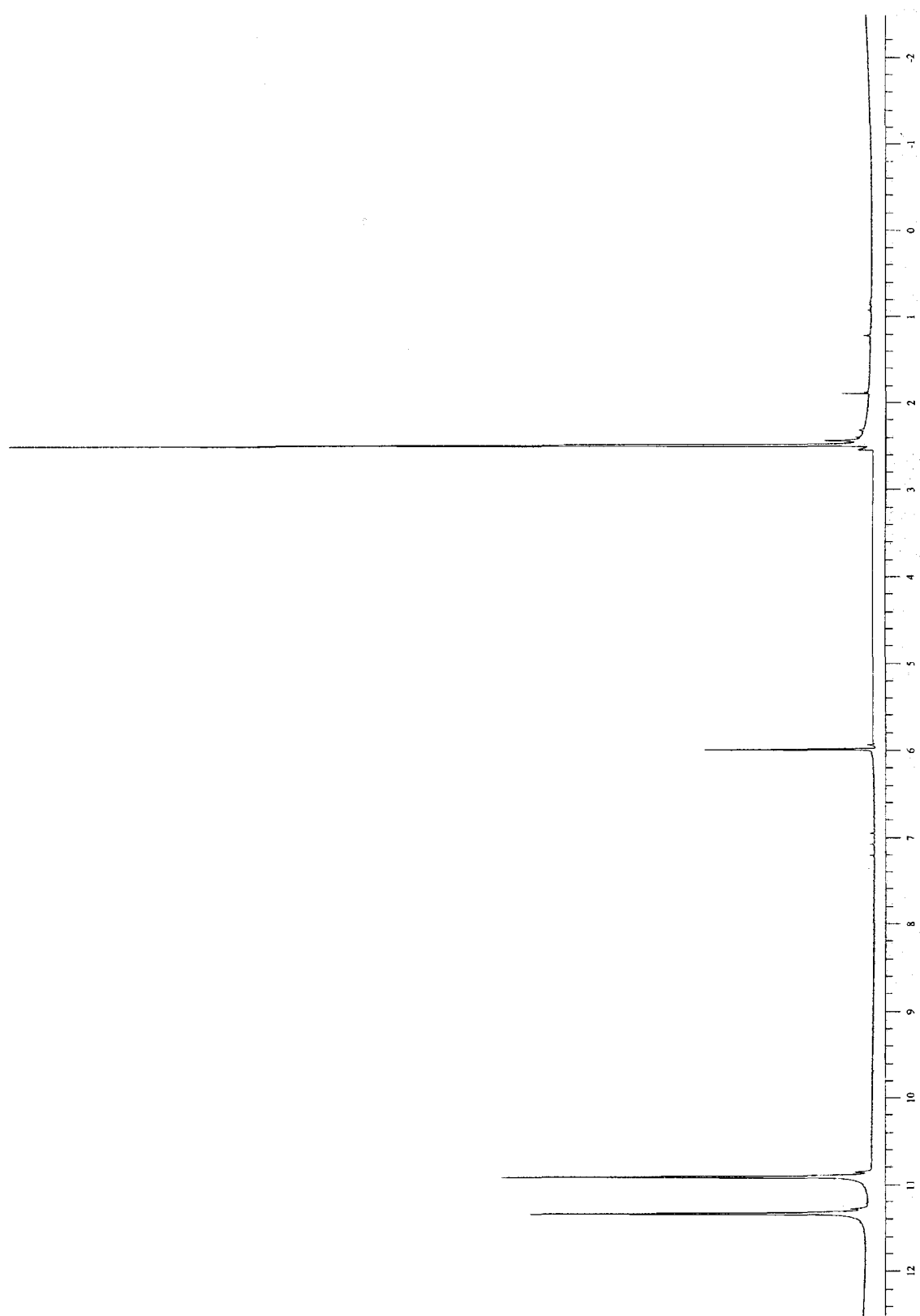doublet (representing ^{1}H5-^{1}H6-OMP).

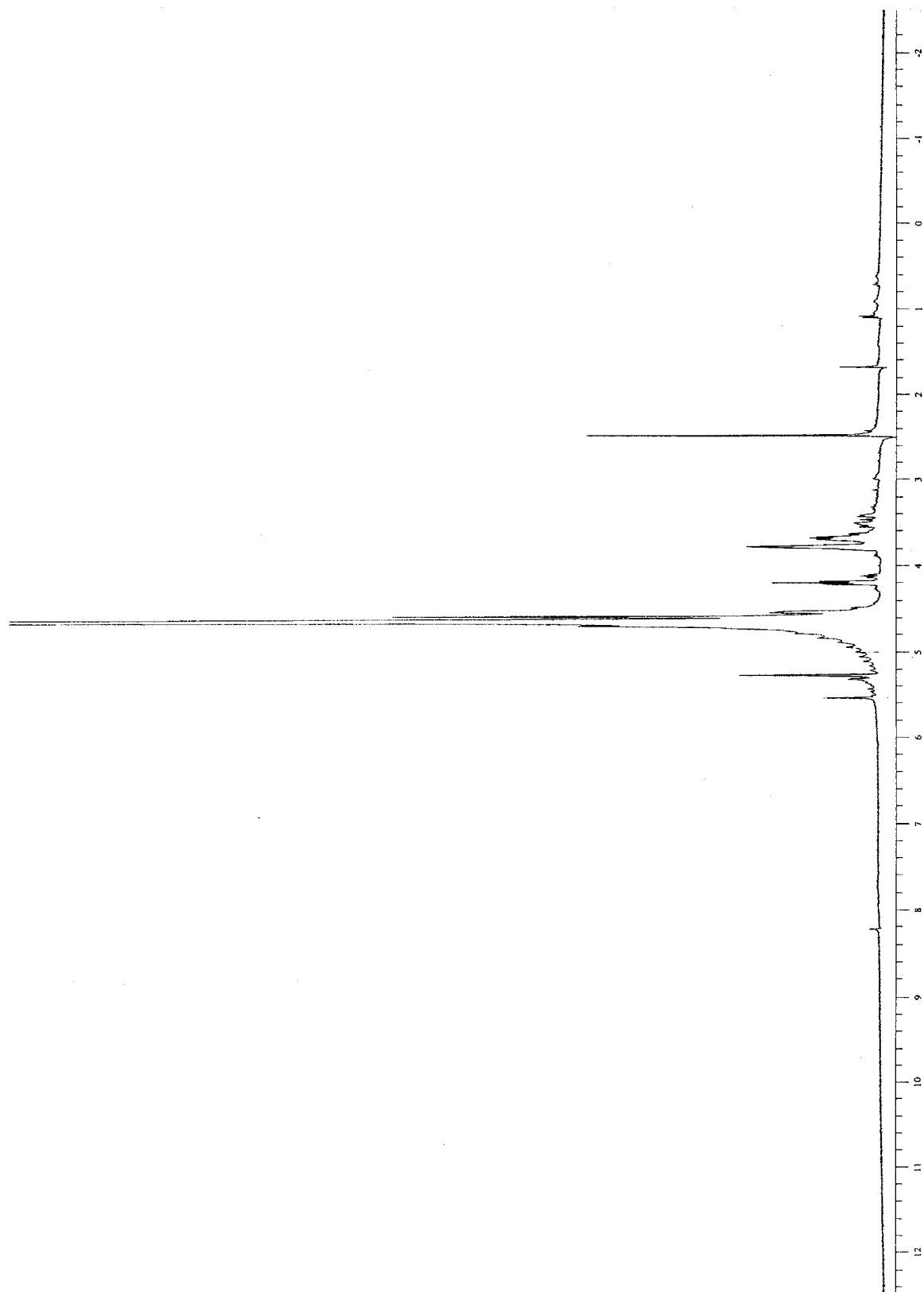Figure 13: ^{1}H NMR of of [5-^{2}H] Orotic Acid.

Figure 14: ^{1}H NMR of [5-^{2}H] Orotidine-5'-Monophosphate.
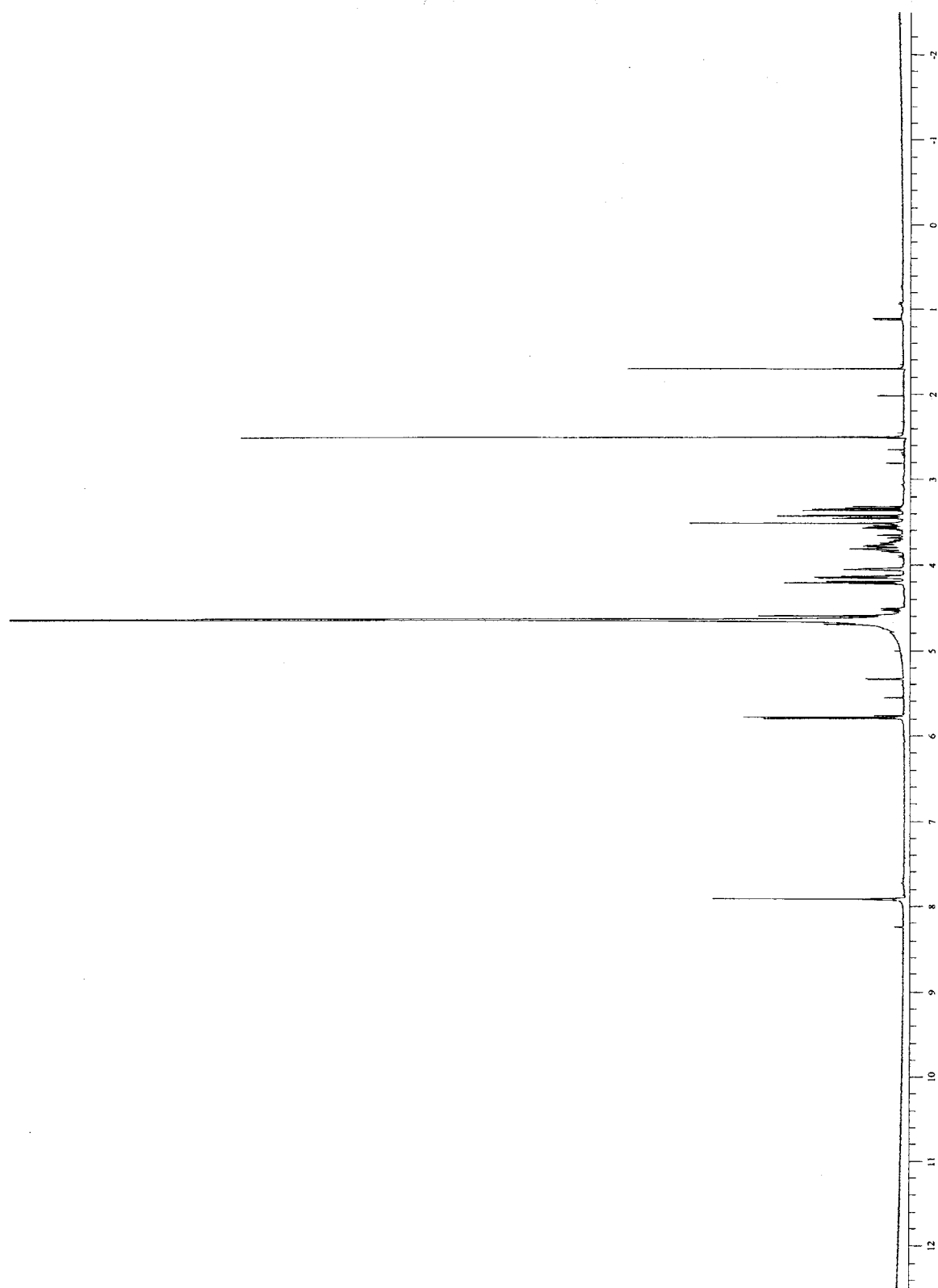
Figure 15: ^{1}H NMR of [5-^{2}H] Uridine-5'-Monophosphate.

Conclusion:

The protocol for the synthesis and purification of both 6-thiocarboxamidouridine-5'monophosphate and ^{15}N-enriched 6-thiocarboxamidouridine-5'monophosphate resulted in stable, isolated ligands as seen by EI-mass spectrometry. These analogues can be used in future experiments in order to provide data on the catalytic mechanism of ODCase.

The purification protocol of ODCase from the yeast strain BJ5424 transformed with plasmid pGU2 yielded ODCase that was free of most protein impurities with only a small, faint band of protein with a slightly larger molecular weight. Purification, using a column containing DEAE Sepharous ion exchange resin, further purified the ODCase as seen in SDS-polyacrylamide gels. ^{1}H NMR data has also shown the apparent ODCase/6-thiocarboxamidouridine-5'monophosphate complex. A singlet, not seen in either ^{1}H NMR of ODCase or 6-thiocarboxamidouridine-5'monophosphate, at 12.3 ppm suggests an apparent coupling of protein and ligand, although the exact molecular site where protonation occurs has yet to be determined. Future studies using experimental techniques, such as Ramen spectroscopy and x-ray crystallization may help provide a bit more insight on the binding orientation occurring within the ODCase active site. Further studies with the synthesized ligand, ^{15}N-enriched 6-thiocarboxamidouridine-5'monophosphate, may provide more information concerning the binding of both analogue and substrate using various NMR techniques.

^{1}H NMR spectra of [5-^{2}H] orotidine-5'-monophosphate resulted in the calculation of 72% deuteration of OMP at the C5 position. The enzymatic decarboxylation of [5-^{2}H] orotidine-5'-monophosphate to [5-^{2}H] uridine-5'-monophosphate shows no change in the integral ratio (H6/(H6+H5+H1')) of signals between both spectra. Rearrangement,

during decarboxylation, would result in a change of the integral ratio and spectra of the substrate and product. Since no change, in either the integral ratio or 1H NMR spectra, can be seen it is concluded no rearrangement between C5 and C6 occurs. A plot of the integral ratio vs. $[(1-f_H) / (2+f_H)]$ x $f_R + f_H / (2+f_H)$ shows a relationship between the integral ratio of UMP and the linear representation for 72% deuterium substitution. According to this plot, the f_R for the integral ratio of 0.44 of [5-^{2}H] uridine-5'-monophosphate is 1.0. A reported $f_R = 1.0$ indicates 100% retention of ^{1}H/^{2}H at the C5 position, thus concluding no rearrangement of protons between the C5 and C6 positions according to our detection methods.

References

1. Jones, M.E. *Annu. Rev. Biochem* **49**, 253-279.

2. Voet, D., Voet, J.G. *Biochemistry 2nd Ed.* (1995), 804.

3. O'Leary, M.H. "The Enzymes", vol. XX. (1992), 235-269.

4. Kluger, R. *Chem. Rev.* **87**, 863.

5. Leussing, D.L., Emly, M. *Adv. Inorg. Biochem.* **4**, 171.

6. Hay, R.W. "Metal Ions in Biological Systems" Vol. 5. (1976), 127. Dekker, New York.

7. Boeker, E.A., Snell, E.E. "The Enzymes" 3rd Ed., Vol. 6. (1972), 217.

8. Braunstein, A.E. "The Enzymes" 3rd Ed., Vol. 9. (1973), 379.

9. Metzler, D.E. *Adv. Enzymol.* **50,** 1.

10. Christen, P., Metzler, D.E. "Transaminases" (1985), Wiley, New York.

11. Vederas, J.C., Floss, H.G. *Acc Chem. Res.* **13**, 455.

12. Hermes, J.D., Tipton, P.A., Fisher, M.A., O'Leary, M.H., Morrion, J.F., Cleland, W.W. *Biochemsitry* **23**, 6263.

13. Silverman, R.B., Groziak, M.P. (1982) *J. Am. Chem. Soc.* 104, 6436-6439.

14. Acheson, S.A., Bell, J.B., Jones, M.E., Wolfenden, R. (1990) *Biochemistry* **29**, 3198-3202.

15. Lee, J.K., Houk, K.N. (1997) *Science* **267**, 942-945.

16. Wolfenden, R., Snider, M., Ridgway, C., Miller, B. (1999) *J. Am. Chem. Soc.* **121**, 7419-7420.

17. Wagner, R., Philipsborn, W.V. (1970) *Helv. Chim. Acta.* **53**, 299.

18. Gawley, R.E., Low, E., Zhang, Q., Harris, R. (2000) *J. Am. Chem. Soc.* **122**, 3344-3350.

19. Appleby, T.C., Kinsland, C., Begley, T.P., Ealick, S.E. (2000) *Proc. Natl. Acad. Sci. USA* **97**, 2005-2010.

20. Beak, P., Siegle, B. (1973) *J. Am. Chem. Soc.* **95**, 7919-7920.

21. Beak, P., Siegle, B. (1976) *J. Am. Chem. Soc.* **98**, 3601-3606.

22. Levin, H.L., Brody, R.S., Westheimer, F.H. (1980) *Biochemistry* **19**, 4699-4706.

23. Shostak, K., Jones, M.E. (1992) *Biochemistry* **31**, 12155-12161.

24. Acheson, S.A., Bell, J.B., Jones, M.E., Wolfenden, R. (1990) *Biochemistry* **29**, 3198-3202.

25. Miller, B.G., Traut, T.W., Wolfenden, R. (1989) *J. Am. Chem. Soc.* **120**, 2666-2667.

26. Smiley, J.A., Jones, M.E. (2000) *Biochemistry* **31**, 12162-12168.

27. Levin, H.L., Brody, R.S., Westheimer, F.H. (1980) *Biochemistry* **19**, 4993-4999.

28. Smiley, J.A., Hay, K.M., Levison, B.S. (2001) *Bioorganic Chemistry* **29**, 96-106.

29. Lue, N.F., Chasman, D.I., Buchman, A.R., Kornberg, R.D. (1987) *Mol. Cell. Biol.* **7**, 3446-3451.

30. Bell, J.B., Jones, M.E. (1991) *J. Biol Chem.* **266**, 12662-12667.

31. Voet, D., Voet, J.G. (1995) *Biochemistry* 2nd *Ed.*, pp. 78-95, John Wiley & Sons, Inc., Somerset, N.J.

32. Creasy, W.A., Handschumacher, R.E. (1961) *J. Biol. Chem.* **236**, 2058-2063.

33. Mishima *et al.* (2000) *J. Am. Chem. Soc.* **122**, 5883-5884.